Clinica Chimica Acta 488 (2019) 68–75

Contents lists available at ScienceDirect

Clinica Chimica Acta

journal homepage: www.elsevier.com/locate/cca

Tissue and serum metabolite profiling reveals potential biomarkers of human hepatocellular carcinoma

Jun Han[a], Wen-xing Qin[b,c], Zhen-li Li[a], Ai-jing Xu[d], Hao Xing[a], Han Wu[a], Han Zhang[a], Ming-da Wang[a], Chao Li[a], Lei Liang[a], Bing Quan[e], Wen-tao Yan[e], Feng Shen[a], Meng-chao Wu[a,*], Tian Yang[a,*]

[a] Department of Hepatobiliary Surgery, Eastern Hepatobiliary Surgery Hospital, Second Military Medical University, Shanghai 200438, China
[b] Department of Clinical Oncology, Changzheng Hospital, Second Military Medical University, Shanghai 200003, China
[c] State Key Laboratory of New Drug & Pharmaceutial Process, Shanghai Institute of Pharmaceutial Industry, Shanghai 200437, China
[d] Department of Infectious Disease, Changhai Hospital, Second Military Medical University, Shanghai 200433, China
[e] Department of Clinical Medicine, Second Military Medical University, Shanghai 200433, China

ARTICLE INFO

Keywords:
Hepatocellular carcinoma
Non-targeted metabolomics
Tissue and serum
Diagnostic ability

ABSTRACT

Background and aims: Metabolomics serves as an important tool in distinguishing changes in metabolic pathways and the diagnosis of human disease. Hepatocellular carcinoma (HCC) is a malignance present of heterogeneous metabolic disorder and lack of effective biomarker for surveillance and diagnosis. In this study, we searched for potential metabolite biomarkers of HCC using tissue and serum metabolomics approach.

Methods: A total of 30 pairs of matched liver tissue samples from HCC patients and 90 serum samples (30 HCC patients, 30 liver cirrhosis patients, and 30 healthy individuals) were assessed. Metabolomics was performed through ultra performance liquid chromatography-mass spectrometry in conjunction with multivariate and univariate statistical analyses.

Results: A total of six differential metabolites including chenodeoxycholic acid (CDCA), glycocholic acid (GCA), LPC20:5, LPE18:0, succinyladenosine and uridine were present in HCC tissue and serum samples. CDCA, LPC20:5, succinyladenosine and uridine were used to construct a diagnostic model based on logistic regression. The four-metabolite panel discriminated HCC from liver cirrhosis with an AUC score of 0.938, sensitivity of 93.3% and specificity of 86.7%. For all HCC and cirrhosis patients, the diagnostic accuracy increased to 96.7% and 90.0%, respectively.

Conclusion: The combination of CDCA, LPC20:5, succinyladenosine and uridine can be used as a biomarker panel to improve HCC sensitivity and specificity. This panel significantly benefits HCC diagnostics and reveals new insight into HCC pathogenesis.

1. Introduction

Primary liver cancer is the sixth most commonly diagnosed cancer and the second leading cause of cancer deaths worldwide [1]. Hepatocellular carcinoma (HCC) is the most common histological type of primary liver cancer that results from chronic hepatitis related liver cirrhosis [2]. HCC has a poor prognosis due to the lack of symptoms during the early stages of the disease. Early discrimination of HCC in high-risk populations can significantly improve HCC survival rates [3].

Currently, diagnostic radiology and serum alpha-fetoprotein (AFP) detection are the two most common approaches for HCC detection [4]. However, diagnostic radiology frequently failed to discriminate small HCC from cirrhotic nodules. For serum samples, AFP produces a 20% false-positive rate in patients with chronic hepatitis and higher rates are detected in patients with liver cirrhosis [5]. Additionally, approximately one-third of HCC patients with small tumors (< 3 cm) show no

Abbreviations: HCC, hepatocellular carcinoma; AFP, alpha-fetoprotein; LC-MS, liquid chromatography-mass spectrometry; HCT, hepatocellular carcinoma tissue; DNT, distal noncancerous tissue; QC, quality control; PCA, principal component analysis; OPLS-DA, orthogonal partial least-squares discriminant analysis; VIP, variable importance in the projection; ROC, receiver operating characteristic; AUC, area under the curve; GCA, glycocholic acid; CDCA, chenodeoxycholic acid; GCDCA, chenodeoxyglycocholic acid

* Corresponding author at: Department of Hepatobiliary Surgery, Eastern Hepatobiliary Surgery Hospital, Second Military Medical University, No. 225, Changhai Road, Shanghai 200438, China.

E-mail addresses: mengchao_wu@sina.com (M.-c. Wu), yangtianehbh@smmu.edu.cn (T. Yang).

https://doi.org/10.1016/j.cca.2018.10.039
Received 25 August 2018; Received in revised form 10 October 2018; Accepted 29 October 2018
Available online 31 October 2018

significant difference in AFP levels when compared to healthy subjects [5]. The limitation of effective diagnostic methods restricts the HCC detection It is therefore imperative to develop a reliable screening method for the early screening of HCC.

Metabolomics is defined as the comprehensive analysis of all metabolites of an isolated organism, cell system, tissue or biological fluid [6]. Tissue metabolomics is the most powerful platform for studying targeted responses to pathogenesis as opposed to changes in the entire metabolic system, and can provide direct information on metabolic modifications and upstream regulations [7,8]. In addition, pairwise comparison of different tissue regions remove individual differences including age and sex [9]. The liver is the metabolic hub of humans and regulate the expression levels of numerous metabolites, thus tissue metabolomics analysis is particularly relevant when assessing HCC occurrence [10]. However, the collection of HCC tissue is invasive, limiting its clinical application. To develop a reliable and non-invasive method for early HCC diagnosis, serum metabolomics still has great potential for biomarker discovery, although its targeting ability and specificity are limited [11–13]. As a consequence, combining tissue and serum metabolomics could facilitate the screening of actual diagnostic biomarkers associated with hepatic pathological changes and HCC development. Nuclear magnetic resonance (NMR), gas chromatography–mass spectrometry (GC–MS), and liquid chromatography-mass spectrometry (LC–MS) are the mostly widely used analytical tools for metabolomics studies [14–16]. LC displays favorable separation of the complex matrix, and MS provides high sensitivity and high resolution for the detection of metabolites. Moreover, separation with LC coupled to MS for detection enables the most comprehensive coverage of metabolites attainable [17].

The primary objective of this study was to identify ideal biomarkers for HCC based on tissue and serum metabolomics using LC–MS. A total of 30 pairs of matched HCC tissues (HCT) and distal noncancerous tissues (DNT) were assessed in combination with 90 serum samples that included healthy controls, liver cirrhosis patients and HCC suffers.

2. Materials and methods

2.1. Participants and the collection of clinical samples

In the present study, a total of 120 participants with tissue and serum samples were recruited between January 2015 and October 2016. Written informed consent was obtained from each participant. The study protocol was approved by the ethics committee of Eastern Hepatobiliary Surgery Hospital and Changhai Hospital. All participants did not receive any treatment or nutrition supplement within 3 months of specimen collection. Detailed information was summarized in Table 1.

Tissues were collected from 30 patients diagnosed with HCC. Two types of liver tissues were obtained from each patient as surgical specimens during the operation including HCTs and DNTs. HCTs were collected from the central area of solid tumor and DNTs were collected 5 cm away from the borders of solid tumors. Serum samples were obtained from 90 participants including 30 healthy individuals, 30 patients with liver cirrhosis and the same 30 patients with HCC. HCC was diagnosed histopathologically, and liver cirrhosis was confirmed through ultrasonic imaging and serum biochemical parameters. Tissue specimens were directly placed into liquid nitrogen after resection. Blood samples were collected prior to surgery, centrifuged within 3 h of collection and stored at −80 °C prior to analysis.

2.2. Tissue pretreatment

Tissue sections A piece of tissue (50 ± 0.5 mg) was mixed with 1.6 mL of prechilled methanol/water (3:1, *v*/v) and homogenized using a Precellys bead beater (5000 Hz, 60 s). Then the sample was placed on ice for 10 min and centrifuged at 4 °C (13,000 rpm for 10 min). The supernatant was transferred and 60 μL internal standards added (L-Phenylalanine-3,3-d_2 30 nmol/mL, Cholic-2,2,4,4-d_4 acid 2 nmol/mL, Lyso PC19:0 2 nmol/mL). The supernatant was dried in Savant vacuum concentrator and then resuspended with 100 μL of methanol/water (3:1, *v*/v). After centrifugation at 4 °C (13,000 rpm for 10 min), the supernatant was collected for analysis.

2.3. Serum pretreatment

A 100 μL aliquot of serum samples added with 30 μL internal standards (L-Phenylalanine-3,3-d_2 30 nmol/mL, Cholic-2,2,4,4-d_4 acid 2 nmol/mL, Lyso PC19:0 2 nmol/mL) was extracted through the addition of 300 μL of methanol, incubation on ice for 10 min and centrifugation at 4 °C (13,000 rpm for 10 min). The supernatant was dried in Savant vacuum concentrator and then resuspended with 50 μL of methanol/water (3:1, *v*/v). After centrifugation at 4 °C (13,000 rpm for 10 min), the supernatant was collected for analysis.

To ensure consistent condition and data quality of the metabolomics, pooled quality control (QC) samples were prepared by mixing all extracted tissues or serum samples for tissue or serum metabolic profiling analysis. The pretreatment of QC samples paralleled with those of the study samples.

2.4. LC–MS analysis

Tissue and serum metabolomics were performed on 30AD UPLC system (Shimadzu, Kyoto, Japan) coupled to a TripleTOF 5600$^+$ mass spectrometer system (AB SCIEX, Framingham, USA). A HSS T3 column

Table 1
Clinical characteristics of all subjects enrolled in tissue and serum set.

	Tissue set		Serum set		
Characteristics	Male	Female	Health	Cirrhosis	HCC
Number	20	10	30	30	30
Age	54 (42–70)	58 (45–68)	58 (40–66)	53 (31–73)	53 (42–70)
Gender (male/female)	20/0	10/0	15/15	23/7	20/10
HBsAg (positive/negative)	18/2	9/1	0/30	28/2	27/3
HCV (positive/negative)	0/20	1/9	0/30	1/29	1/29
AFP (ng/mL) > 20/ < 20	8/12	5/5	0/30	7/23	13/17
ALT (U/L)	27 (15–65)	37.5 (15–83)	21 (11 − 32)	37 (12–160)	35 (15–83)
AST (U/L)	37.5 (19–60)	35 (14–90)	17.5 (13–35)	28.5 (12–79)	37 (14–90)
Tumor diameter (cm)					
≤3	6	3	–	–	9
3–5	4	3	–	–	7
5–10	5	2	–	–	7
> 10	5	2	–	–	7

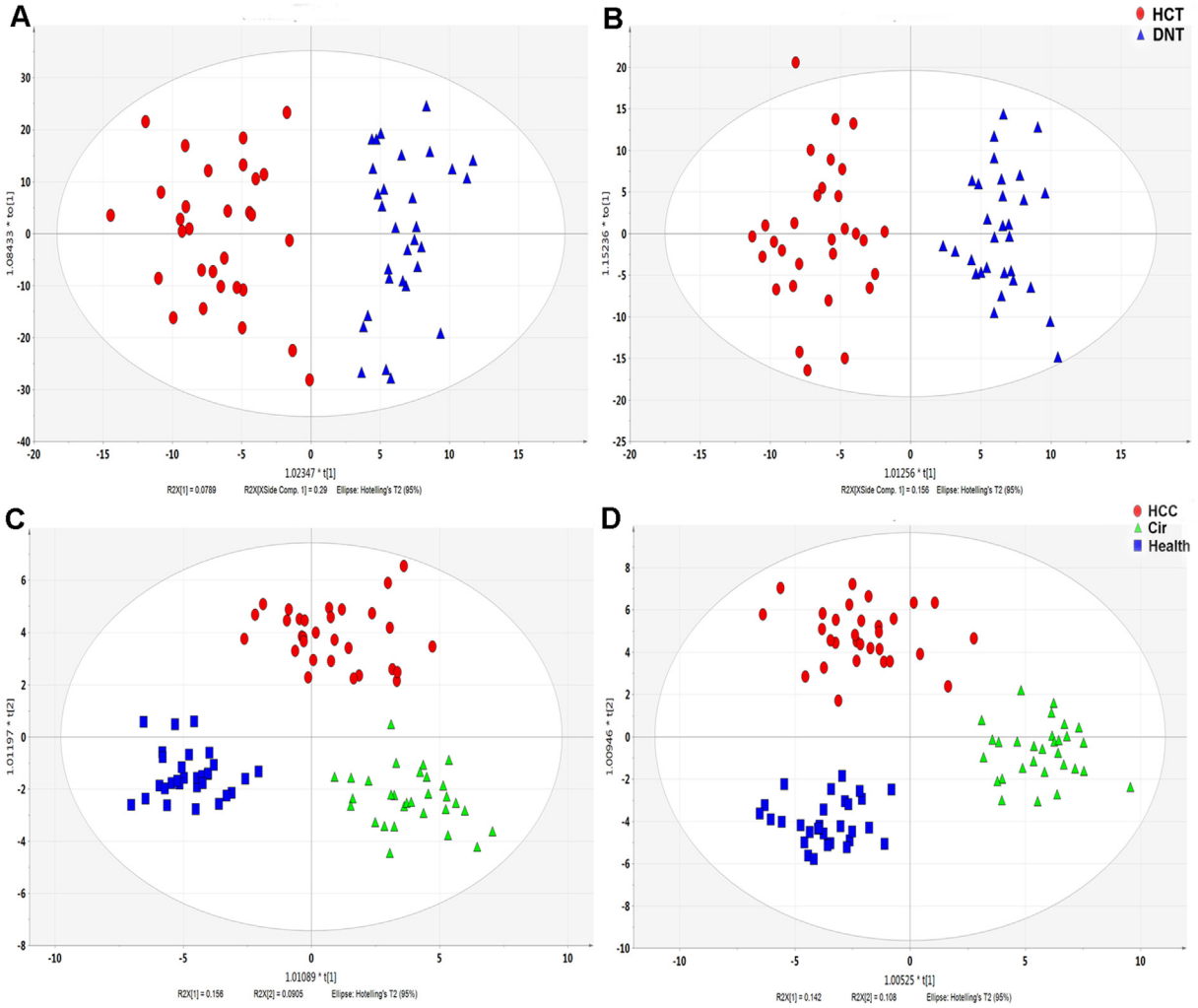

Fig. 1. OPLS-DA plot score showed a global metabolic difference between the groups. (A) HCT and DNT, ESI + mode (B) HCT and DNT, ESI- mode (C) Healthy control, cirrhosis and HCC serum, ESI + mode (D) Healthy control, cirrhosis and HCC serum, ESI- mode.

(100 mm × 2.1 mm, 1.8 μm, Waters) was used for analysis. The mobile phase A was water (0.1% formic acid) and B was methanol (0.1% formic acid). The gradient program was: 0–2 min 5% B, 2–10 min 5%–75% B, 10–22 min 75%–100% B, 22–27 min 100% B, 27–27.5 min 100%–5% B, 27.5–30 min 5% B. The flow rate was 0.35 mL/min and column oven set to 40 °C. A 5 μL of sample was loaded for each individual analysis and the sample sequence was random. Scan range of mass spectrum was collected between 50 and 1000 *m/z*. The ion spray voltage was set at 5500 V in the ESI^+ mode and −4500 V in the ESI^- mode. The capillary temperature was maintained at 550 °C. The collision energy was set to 10, 20, or 40 V in the ESI^+ mode and −10, −20, or −40 V in the ESI^- mode according to the requirement. All the samples were kept at 4 °C during analysis.

2.5. Data processing and statistical analysis

The processed data was uploaded to SIMCA-P 14.1 (Umetrics AB, Umea, Sweden) for multivariate analysis. An unsupervised model of the principal component analysis (PCA) was applied to monitor study stability and the supervised model of orthogonal partial least-squares discriminant analysis (OPLS-DA) was used to maximize the distance between different groups with the contribution to classification according to variable importance in the projection (VIP).

Univariate statistical analysis was preformed to assess statistical significance, and Receiver operating characteristic (ROC) curve and the binary logistic regression were used to evaluate the diagnostic ability via SPSS 24.0 software (IBM, Armonk, USA).

Structural information was well matched to those of authentic standards or confirmed spectra in the Human Metabolome Database (http://www.hmdb.ca/), METLIN (http://metlin.scripps.edu/index.php) or Lipidmaps (http://www.lipidmaps.org). MultiExperiment Viewer software 4.6.2 (http://www.tm4.org/) was used to generate heat maps of differential metabolites.

3. Results

3.1. Reliability of analytical methods

Tissue and serum metabolic profiling were performed separately and samples in each set was analyzed in a random order. Pooled QC samples were inserted into the two sequences to evaluate analytical stability. In PCA score plots, QC samples in tissue (Supplementary Fig. S1 A–B) and serum sets (Supplementary Fig. S1 C–D) were clustered in the ESI + and ESI- modes indicating good reproducibility. In addition, variations in retention time, mass accuracy, and peak areas in QC samples were calculated. The retention time shift was < 0.3 min and the mass accuracy deviation was < 5 mDa. The relative standard deviations (RSD) of peak areas were below 30%.

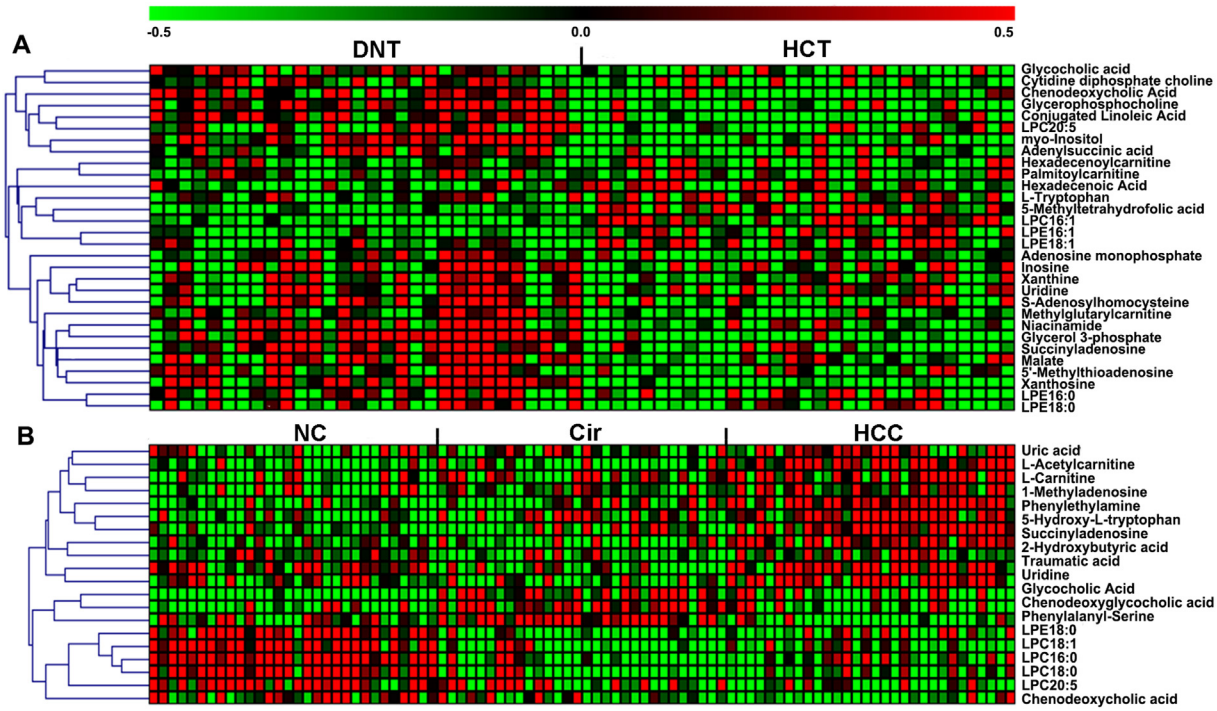

Fig. 2. Heat map of the differential metabolites. The colors on the heat map were determined by the *Z*-score, reflecting the relative concentrations. The red and green colors indicate relatively higher and lower concentrations (A) DNT and HCT group in tissue set; (B) Healthy control, liver cirrhosis and HCC group in serum. (For interpretation of the references to colour in this figure legend, the reader is referred to the web version of this article.)

3.2. Metabolomics of liver tissues

All 30 pairs of HCTs and DNTs were compared to explore direct metabolic changes in the liver. Supervised multivariate models of OPLS-DA revealed a clear separation of the two tissue types both in the ESI+ and ESI- modes with two components (Fig. 1A–B). As illustrated by the OPLS-DA score plots, the model parameters of $R^2Y(cum)$ and $Q^2(cum)$ were 0.85 and 0.721 in the ESI+ mode, and 0.898 and 0.824 in the ESI- mode, representing the favorable evaluation of the fitness and prediction ability of OPLS-DA model. Subsequently, permutation tests repeated 100 times were performed to validate the reliability of the model and no over-fitting were observed as the permuted R^2 and Q^2 values to the left were lower than the original points to the right, and the intercept of Q^2 was below zero (Supplementary Fig. S2) [18]. Metabolites that differentiate HCT from DNT were selected according to VIP values, and variables with a VIP > 1.0 were retained and recognized as statistical importance on the classification [19]. Then, univariate test ($P < 0.05$) was applied to identify differentially expressed metabolites by comparison between HCT and DNT group. Ultimately, a total of 30 candidate metabolites were identified (Supplementary Table S1).

To assess the overall impact of the 30 metabolites, heat maps were constructed based on Pearson correlation coefficients (Fig. 2A). Compared to DNTs, HCTs had relatively lower levels of metabolites that participated in glycerophospholipid metabolism (glycerol 3-phosphate, glycerophosphocholine, LPC20:5, LPE16:0, LPE18:0), purine metabolism (uridine, xanthine, xanthosine, adenosine monophosphate, succinyladenosine, inosine), bile acid metabolism (glycocholic acid (GCA) and chenodeoxycholic acid (CDCA)), together with higher levels of long-chain carnitines (hexadecenoylcarnitine, palmitoylcarnitine) and several glycerophospholipid and fatty acid molecules (LPC16:1, LPE16:1, LPE18:1, hexadecenoic acid).

3.3. Metabolomics of health, cirrhosis and HCC serum

To further confirm the metabolic variations during HCC progression, 90 serum samples (including 30 patients with HCC, 30 patients with liver cirrhosis, and 30 healthy controls) were assessed using identical methods. OPLS-DA was also performed to discriminate HCC, healthy and cirrhotic groups (Fig. 1C–D). The cumulative R^2Y and Q^2 values were 0.864 and 0.798 in the ESI+ mode, and 0.879 and 0.788 in the ESI- mode, respectively. After screening for VIP values > 1.0, a univariate test ($P < 0.05$) was applied to identify differentially expressed metabolites by pairwise comparisons: HCC versus healthy controls and cirrhosis, respectively. Each significantly altered metabolite was enrolled for identification and 19 candidates were ultimately obtained (Supplementary Table S2). A heat map was generated to visualize the relative levels in the three groups (Fig. 2B). Compared to the other two groups, uric acid, L-acetylcarnitine, L-carnitine, 1-methyladenosine, phenylethylamine, 5-hydroxy-L-trypophan, succinyladenosine, 2-hydroxybutyric acid, traumatic acid and uridine had relatively higher concentrations in the HCC group. GCA, chenodeoxyglycocholic acid (GCDCA) and phenylalanyl-serine displayed higher levels in the cirrhosis group, whilst CDCA and several glycerophospholipids displayed elevated levels in the healthy group.

3.4. Defining of potential metabolic biomarkers for HCC

We identified six differential metabolites (CDCA, GCA, LPC20:5, LPE18:0, succinyladenosine and uridine) that were both present in tissue and serum samples (Fig. 3A–F). A stepwise logistic regression model for HCC diagnosis was employed to construct a model based on these metabolites on serum data set. CDCA, LPC20:5, succinyladenosine and uridine were found to be the most significant predictors (Supplementary Table S3). This metabolite panel for the detection of HCC was constructed as follows: logit [P = HCC] = 10.201 × [succinyladenosine]-11.1 × [LPC20:5] + 17.923 × [uridine]-3.65 × [CDCA]. The panel displayed greater diagnostic performance than AFP when comparing HCC to non-HCC at the optimal cut-off values (Fig. 4A, Table 2), with an AUC score of 0.962 versus 0.703, a sensitivity of 96.7% versus 53.3% and a specificity of 88.3% versus 83.3%, respectively. When HCC was compared to cirrhosis (Fig. 4B, Table 2), the panel displayed

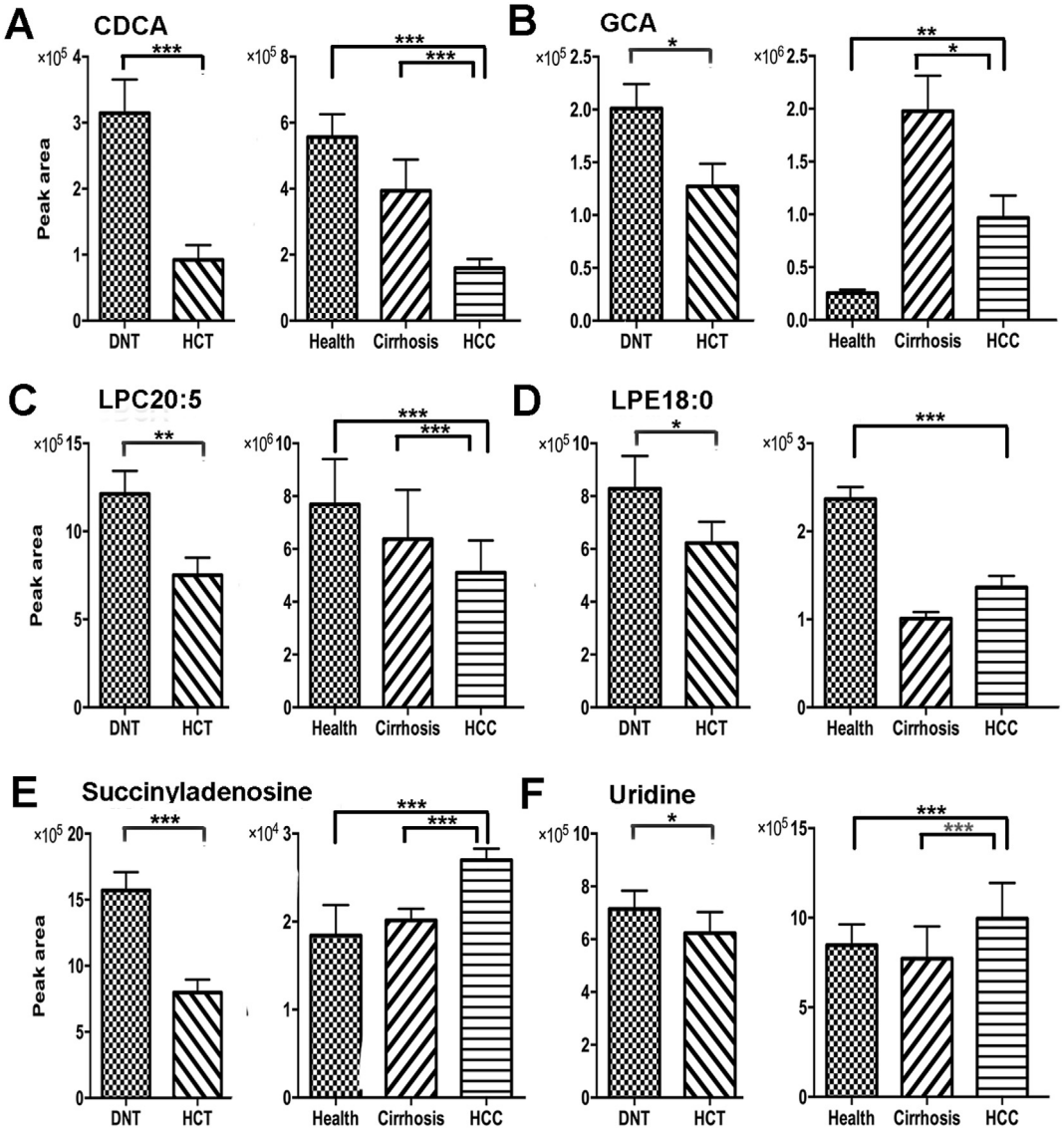

Fig. 3. Concentrations of CDCA, GCA, LPC20:5, LPE18:0, succinyladenosine and uridine in tissue and serum samples. $*p < 0.05$, $**p < 0.01$, and $***p < 0.001$.

improved diagnostic ability with an AUC score of 0.938 versus 0.656, a sensitivity of 93.3% versus 53.3% and a specificity of 86.7% versus 76.7%, respectively. The predicted probability of being diagnosed with HCC from the logistic model is shown in Fig. 4C. At the traditional cutoff values (0.5) [11], 100%, 93.3% and 90% of healthy controls, cirrhosis and HCC subjects were correctly discriminated from the serum samples. Of value, for all HCC and cirrhosis patients, the diagnostic accuracies were 96.7% and 90.0%, respectively. For false-negative (AFP < 20 ng/mL) AFP patients with HCC and AFP false-positive (AFP > 20 ng/mL) patients with liver cirrhosis, the diagnostic accuracy was 85.7% and 85.7%, respectively (Fig. 4D).

4. Discussion

A great deal of attention has focused on the clinical application of systems biology platforms. Metabolomics aims to assess the altered activity of cellular state and enzymes, and changes in metabolic reactions [20–22]. Compared to other omic approaches, metabolomics more closely correlates to phenotypic changes and can serve as a translational research tool that bridges clinical and basic science during cancer diagnosis [23,24].

A total of 6 metabolites were identified both in tissue and serum samples. Purine metabolism, bile acid synthesis and glycerophospholipid metabolism displayed the greatest variation and were closely associated with HCC development (Fig. 3). Purines are the most abundant metabolic products due to their requirement for nuclei acid synthesis, and their roles as cofactors that promote cell proliferation and survival [25]. Cellular purine levels are maintained through the coordination of salvage and de novo biosynthetic pathways, the latter being enhanced in tumor cells as purine nucleotides are required for tumor cell proliferation [26]. Emerging evidence also demonstrates the importance of purine metabolism in immune defenses and the tumor microenvironment through their ability to regulate P2X ligand-gated ion channels and G protein-coupled P2Y receptors [26,27]. Targeting purine metabolism therefore has potential during cancer therapy.

Bile acids, initially known for their role in lipid and vitamin metabolism, are now recognized as crucial molecules involved in cross tissue signaling, particularly in the liver and during gut microbiome crosstalk [28,29]. Both protective and pathogenic roles of bile acids have been identified, including non-alcoholic steatohepatitis, colon cancer and HCC [30,31]. Although the precise effects of bile acids on hepatocarcinogenesis remain largely unknown, an increasing number of studies have demonstrated that their accumulation in hepatocytes leads to cytotoxicity by inducing the formation of reactive oxygen species

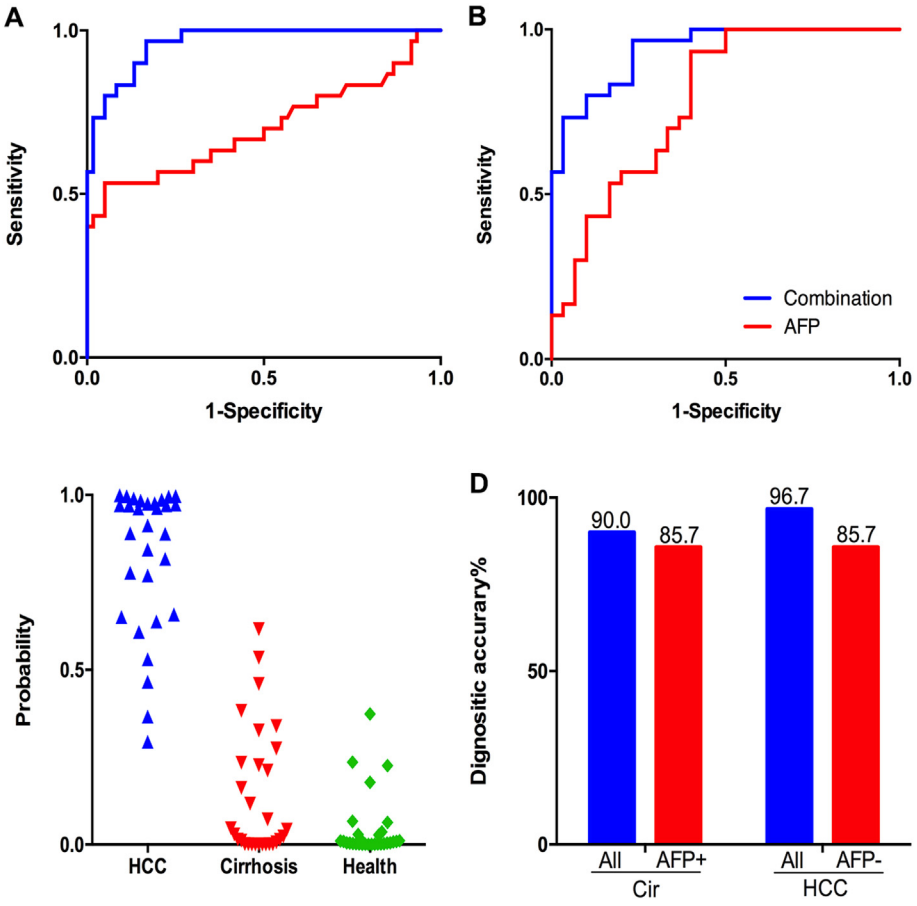

Fig. 4. Diagnostic potential of CDCA, LPC20:5, succinyladenosine and uridine in HCC serum. (A). ROC curves to distinguishing HCC patients from non-HCC patients. (B). ROC curves to distinguishing HCC patients from cirrhosis patients. (C) Discrimination of HCC, cirrhosis and healthy controls at a cut-off of 0.5 (D) Diagnostic accuracy in HCC, cirrhosis, false diagnosed patients by AFP. AFP+: false positive AFP (cirrhosis patients with AFP > 20 ng/mL), AFP-: false negative AFP (HCC patients with AFP < 20 ng/mL).

Table 2
ROC analysis for serum samples.

		Metabolites	AUC	Standard error	95% CI		Sensitivity (%)	Specificity (%)
					Lower	Upper		
Serum set	HCC vs non-HCC	CDCA	0.831	0.047	0.74	0.923	95.0	60.0
		LPC20:5	0.833	0.043	0.75	0.917	85.0	66.7
		Succinyladenosine	0.851	0.043	0.766	0.936	80.0	79.3
		Uridine	0.769	0.055	0.661	0.867	76.7	75.0
		AFP	0.703	0.067	0.572	0.834	53.3	83.3
		Combined	0.962	0.017	0.929	0.995	96.7	88.3
	HCC vs Cirrhosis	CDCA	0.786	0.059	0.67	0.902	93.3	60.0
		LPC20:5	0.771	0.059	0.655	0.888	73.3	70.0
		Succinyladenosine	0.806	0.059	0.690	0.921	80.0	76.6
		Uridine	0.794	0.058	0.681	0.908	76.7	80.0
		AFP	0.656	0.074	0.51	0.801	53.3	76.7
		Combined	0.938	0.028	0.883	0.993	96.7	86.7

(ROS), ultimately leading to apoptosis or necrosis [32,33]. Dysbiosis (microbial imbalance) or elevated levels of bile acids in circulation may produce numerous cellular disorders, leading to sustained liver injury [34]. An important determinant of the biological effects of a particular bile acid is hydrophobicity [35]. Excessive production of hydrophobic bile acids is cytotoxic and promotes hepatocyte injury [36]. Hydrophilic bile acids differ in their physicochemical and biological characteristics and are thought to be hepatoprotective [37,38]. In this study, in addition to CDCA and GCA, GCDCA levels were altered in HCC serum. GCA and GCDCA are highly hydrophobic and were present in high levels in cirrhosis and HCC group. In contrast, CDCA, as high hydrophilic bile acid, reduced from health controls, cirrhosis to HCC group, indicating the protective function during carcinogenesis. However, the levels of all three bile acids were observed decreased in HCC tumor tissues, and it suggests that cancer cells utilize to escape immune attack and apoptotic cell death, given that bile acids act as mediators in regulating immune and inflammation [32,35].

Lipid metabolism is a key molecular integrator of energy homeostasis, membrane structure, and signaling. Accordingly, its dysregulation contributes to diverse phenotypes [39,40]. Lysophospholipids are potent bioactive lipids that accounted for the majority of identified tissue and serum metabolites including several LPCs and LPEs (Supplementary Table S1, 2). Almost all metabolomics studies reported an imbalance of lysophospholipids, however, relatively little is known about their role underlying the progression of HCC [41]. Recent studies showed that LPC promotes cell viability within the tumor vascular endothelium through phosphatidylinositol 3-kinase/Akt pathway [42–44]. And plasma LPC concentration are lower in cancer patients

due to their activated inflammatory status [42]. We identified four LPCs in serum with reduced level in HCC patients. But, different kinds of LPCs were variable in HCC tissues. Thus, it is considered that a variety of LPCs participate in different biological processes that promote HCC development. Another major lysophospholipid of LPE has been revealed to regulate intercellular signaling through putative G protein-coupled receptors (GPCRs) [45,46]. Like LPCs, LPEs displays the major biofunction via transformation to LPA and were observed variability across HCC tissues (Supplementary Table S1) [47]. The role of lysophospholipids during HCC development has not been described in detail and now warrants further investigation.

Ultimately, CDCA bile acids, LPC20:5 lysophospholipids and the purine metabolites succinyladenosine and uridine were selected as candidate biomarkers. Independent assessment of CDCA, LPC 20:5, succinyladenosine and uridine levels could more accurately diagnose HCC when compared to AFP (Table 2). However, the specificity of CDCA, LPC20:5, succinyladenosine and uridine alone were 60%, 66.7%, 79.3% and 75.0%. Thus, the metabolites were combined to establish a diagnostic model that showed excellent AUC scores, sensitivity and the specific ability to discriminate HCC, non-HCC and cirrhosis patients. The four-metabolite model also raised the diagnostic accuracy of all HCC and cirrhosis patients to 96.7% and 90.0%, respectively. For AFP false-negative HCC patients and AFP false-positive liver cirrhosis patients, the diagnostic accuracy reached 85.7% and 85.7%, respectively (Fig. 4A–D). Previous studies have identified biomarkers with high AUC score, sensitivity and specificity. A panel of palmitoylcarnitine and L-arginine was identified with an AUC score of 0.988, sensitivity of 97.3% and specificity of 100% to discriminate HCC from liver cirrhosis [48]. Another panel of canavaninosuccinate and AFP was reported to display a sensitivity of 96.4% and specificity of 100% for HCC diagnosis [12]. However, it's not clear whether the variation of palmitoylcarnitine, L-arginine and canavaninosuccinate was associated with HCC, for they were not unique to hepatocyte or validated in HCC tissues. Thus, as CDCA, LPC20:5, succinyladenosine and uridine levels were validated in both HCC tissue and serum, their correlation to HCC development is more convincing.

In summary, metabolomics can improve cancer diagnosis and increase our understanding of tumor biology. Measurement of CDCA, LPC 20:5, succinyladenosine and uridine in tissue and serum samples can discriminate HCC from liver cirrhosis with improved sensitivity and specificity than AFP. We therefore demonstrate metabolomics as a promising screening tool for HCC biomarkers. The power of these biomarkers in the clinic now requires confirmation in large-scale and multicenter cohorts.

Conflicts of interest

The authors have no conflicts of interest to declare.

Grant support

This work was supported in part by the National Natural Science Foundation of China (No. 81472284 and 81672699).

Authors' contributions

Jun Han, Wen-xing Qin, Zhen-li Li, Ai-jing Xu and Hao Xing contributed equally to this work.

Appendix A. Supplementary data

Supplementary data to this article can be found online at https://doi.org/10.1016/j.cca.2018.10.039.

References

[1] K.A. McGlynn, J.L. Petrick, W.T. London, Global epidemiology of hepatocellular carcinoma an emphasis on demographic and regional variability, Clin. Liver Dis. 19 (2) (2015) 223–238.
[2] H.B. El-Serag, K.L. Rudolph, Hepatocellular carcinoma: epidemiology and molecular carcinogenesis, Gastroenterology 132 (7) (2007) 2557–2576.
[3] M. Sakamoto, Early HCC: diagnosis and molecular markers, J. Gastroenterol. 44 (Suppl. 19) (2009) 108–111.
[4] A. Colli, M. Fraquelli, G. Casazza, et al., Accuracy of ultrasonography, spiral CT, magnetic resonance, and alpha-fetoprotein in diagnosing hepatocellular carcinoma: a systematic review, Am. J. Gastroenterol. 101 (3) (2006) 513–523.
[5] L. Chen, D.W. Ho, N.P. Lee, et al., Enhanced detection of early hepatocellular carcinoma by serum SELDI-TOF proteomic signature combined with alpha-fetoprotein marker, Ann. Surg. Oncol. 17 (9) (2010) 2518–2525.
[6] U. Roessner, J. Bowne, What is metabolomics all about, BioTechniques 46 (5) (2009) 363–365.
[7] Y. Lu, N. Li, L. Gao, et al., Acetylcarnitine is a Candidate Diagnostic and Prognostic Biomarker of Hepatocellular Carcinoma, Cancer Res. 76 (10) (2016) 2912–2920.
[8] C.H. Johnson, J. Ivanisevic, G. Siuzdak, Metabolomics: beyond biomarkers and towards mechanisms, Nat. Rev. Mol. Cell Biol. 17 (7) (2016) 451–459.
[9] S. Naz, dSDC Moreira, A. García, C. Barbas, Analytical protocols based on LC-MS, GC-MS and CE-MS for nontargeted metabolomics of biological tissues, Bioanalysis 6 (12) (2014) 1657–1677.
[10] T. Kimhofer, H. Fye, S. Taylor-Robinson, et al., Proteomic and metabonomic biomarkers for hepatocellular carcinoma: a comprehensive review, Br. J. Cancer 112 (7) (2015) 1141–1156.
[11] J. Zeng, P. Yin, Y. Tan, et al., Metabolomics study of hepatocellular carcinoma: discovery and validation of serum potential biomarkers by using capillary electrophoresis-mass spectrometry, J. Proteome Res. 13 (7) (2014) 3420–3431.
[12] B. Wang, D. Chen, Y. Chen, et al., Metabonomic profiles discriminate hepatocellular carcinoma from liver cirrhosis by ultraperformance liquid chromatography-mass spectrometry, J. Proteome Res. 11 (2) (2012) 1217–1227.
[13] T. Chen, G. Xie, X. Wang, et al., Serum and urine metabolite profiling reveals potential biomarkers of human hepatocellular carcinoma, Mol. Cell. Proteomics 10 (7) (2011) M110.004945.
[14] L. Zhou, L. Ding, P. Yin, et al., Serum metabolic profiling study of hepatocellular carcinoma infected with hepatitis B or hepatitis C virus by using liquid chromatography-mass spectrometry, J. Proteome Res. 11 (11) (2012) 5433–5442.
[15] Y. Liu, Z. Hong, G. Tan, et al., NMR and LC/MS-based global metabolomics to identify serum biomarkers differentiating hepatocellular carcinoma from liver cirrhosis, Int. J. Cancer 135 (3) (2014) 658–668.
[16] R.M.R. Nezami, Y. Luo, P.C. Di, et al., GC-MS based plasma metabolomics for identification of candidate biomarkers for hepatocellular carcinoma in Egyptian cohort, PLoS ONE 10 (6) (2015) e0127299.
[17] P. Yin, D. Wan, C. Zhao, et al., A metabonomic study of hepatitis B-induced liver cirrhosis and hepatocellular carcinoma by using RP-LC and HILIC coupled with mass spectrometry, Mol. BioSyst. 5 (8) (2009) 868–876.
[18] S. Mahadevan, S. Shah, T. Marrie, et al., Analysis of metabolomic data using support vector machines, Anal. Chem. 80 (19) (2008) 7562–7570.
[19] E.C. Chan, K.K. Pasikanti, J.K. Nicholson, Global urinary metabolic profiling procedures using gas chromatography-mass spectrometry, Nat. Protoc. 6 (10) (2011 Sep 8) 1483–1499.
[20] J.L. Griffin, J.P. Shockcor, Metabolic profiles of cancer cells, Nat. Rev. Cancer 4 (7) (2004) 551–561.
[21] P. Mendes, D.B. Kell, H.V. Westerhoff, Why and when channelling can decrease pool size at constant net flux in a simple dynamic channel, Biochim. Biophys. Acta 1289 (2) (1996) 175–186.
[22] P. Mendes, D.B. Kell, H.V. Westerhoff, Channelling can decrease pool size, Eur. J. Biochem. 204 (1) (1992) 257–266.
[23] J.K. Nicholson, J.C. Lindon, E. Holmes, 'Metabonomics': understanding the metabolic responses of living systems to pathophysiological stimuli via multivariate statistical analysis of biological NMR spectroscopic data, Xenobiotica 29 (11) (1999) 1181–1189.
[24] J.L. Spratlin, N.J. Serkova, S.G. Eckhardt, Clinical applications of metabolomics in oncology: a review, Clin. Cancer Res. 15 (2) (2009) 431–440.
[25] J. Yin, W. Ren, X. Huang, et al., Potential mechanisms connecting purine metabolism and cancer therapy, Front. Immunol. 9 (2018 Jul 30) 1697.
[26] A.M. Pedley, S.J. Benkovic, A new view into the regulation of purine metabolism: The purinosome, Trends Biochem. Sci. 42 (2) (2017 Feb) 141–154.
[27] M. Idzko, Purines in tissue inflammation and fibrosis, Purinergic Signal 10 (2014) 726.
[28] R.M. Gadaleta, S.W. van Mil, B. Oldenburg, et al., Bile acids and their nuclear receptor FXR: Relevance for hepatobiliary and gastrointestinal disease, Biochim. Biophys. Acta 1801 (7) (2010) 683–692.
[29] L. Sun, K. Beggs, P. Borude, et al., Bile acids promote diethylnitrosamine-induced hepatocellular carcinoma via increased inflammatory signaling, Am. J. Physiol. Gastrointest. Liver Physiol. 311 (1) (2016) G91–91G104.
[30] J.Y. Chiang, Bile acid metabolism and signaling, Compr. Physiol. 3 (3) (2013) 1191–1212.
[31] I. Kim, K. Morimura, Y. Shah, et al., Spontaneous hepatocarcinogenesis in farnesoid X receptor-null mice, Carcinogenesis 28 (5) (2007) 940–946.
[32] M.J. Perez, O. Briz, Bile-acid-induced cell injury and protection, World J. Gastroenterol. 15 (14) (2009) 1677–1689.
[33] G. Xie, X. Wang, F. Huang, et al., Dysregulated hepatic bile acids collaboratively

promote liver carcinogenesis, Int. J. Cancer 139 (8) (2016) 1764–1775.
[34] J.R. Swann, E.J. Want, F.M. Geier, et al., Systemic gut microbial modulation of bile acid metabolism in host tissue compartments, Proc. Natl. Acad. Sci. U. S. A. 108 (Suppl. 1) (2011) 4523–4530.
[35] B. Sánchez, Bile acid-microbiota crosstalk in gastrointestinal inflammation and carcinogenesis: a role for bifidobacteria and lactobacilli, Nat. Rev. Gastroenterol. Hepatol. 15 (4) (2018) 205.
[36] J.D. Amaral, R.J. Viana, R.M. Ramalho, et al., Bile acids: Regulation of apoptosis by ursodeoxycholic acid, J. Lipid Res. 50 (9) (2009) 1721–1734.
[37] J.J. Marin, R.I. Macias, O. Briz, et al., Bile acids in physiology, pathology and pharmacology, Curr. Drug Metab. 17 (1) (2015) 4–29.
[38] M. Xu, Q. Zhao, D. Shao, et al., Chenodeoxycholic acid derivative HS-1200 inhibits hepatocarcinogenesis and improves liver function in diethylnitrosamine-exposed rats by downregulating MTH1, Biomed. Res. Int. 2017 (2017) 1465912.
[39] M.R. Wenk, Lipidomics: new tools and applications, Cell 143 (6) (2010) 888–895.
[40] N.J. Skill, R.E. Scott, J. Wu, M.A. Maluccio, Hepatocellular carcinoma associated lipid metabolism reprogramming, J. Surg. Res. 169 (1) (2011) 51–56.
[41] A. Mazzocca, F. Dituri, L. Lupo, et al., Tumor-secreted lysophostatidic acid accelerates hepatocellular carcinoma progression by promoting differentiation of peritumoral fibroblasts in myofibroblasts, Hepatology 54 (3) (2011) 920–930.
[42] L.A. Taylor, J. Arends, A.K. Hodina, et al., Plasma lyso-phosphatidylcholine concentration is decreased in cancer patients with weight loss and activated inflammatory status, Lipids Health Dis. 6 (2007) 17.
[43] A. Linkous, L. Geng, A. Lyshchik, et al., Cytosolic phospholipase A2: targeting cancer through the tumor vasculature, Clin. Cancer Res. 15 (5) (2009) 1635–1644.
[44] Y. Fujita, M. Yoshizumi, Y. Izawa, et al., Transactivation of fetal liver kinase-1/kinase-insert domain-containing receptor by lysophosphatidylcholine induces vascular endothelial cell proliferation, Endocrinology 147 (3) (2006) 1377–1385.
[45] K.S. Park, H.Y. Lee, S.Y. Lee, et al., Lysophosphatidylethanolamine stimulates chemotactic migration and cellular invasion in SK-OV3 human ovarian cancer cells: involvement of pertussis toxin-sensitive G-protein coupled receptor, FEBS Lett. 581 (23) (2007) 4411–4416.
[46] S.J. Park, K.P. Lee, S. Kang, et al., Lysophosphatidylethanolamine utilizes LPA and CD97 in MDA-MB-231 breast cancer cells, Cell. Signal. 25 (11) (2013) 2147–2154.
[47] J.M. Lee, S.J. Park, D.S. Im, Calcium Signaling of Lysophosphatidylethanolamine through LPA1 in Human SH-SY5Y Neuroblastoma Cells, Biomol. Ther. (Seoul) 25 (2) (2017) 194–201.
[48] Lu Y, C. Huang, L. Gao, et al., Identification of serum biomarkers associated with hepatitis B virus-related hepatocellular carcinoma and liver cirrhosis using mass-spectrometry-based metabolomics, Metabolomics 11 (6) (2015) 1526–1538.